Revista de Metalurgia
Vol. 53, Issue 4, October–December 2017, e104
ISSN-L: 0034-8570
doi: http://dx.doi.org/10.3989/revmetalm.104

Experimental characterization of nanoparticles emissions during Laser Shock Processing of AA6061, AISI304 and Ti6Al4V

João F. Gomes[a,b,✉], Rosa M. Miranda[c], Juan A. Porro[d], José L. Ocaña[d]

[a] ISEL – Instituto Superior de Engenharia de Lisboa, Área Departamental de Engenharia Química, Rua Conselheiro Emídio Navarro 1, 1959-007 Lisboa, Portugal

[b]CERENA – Centro de Recursos Naturais e Ambiente, Instituto Superior Técnico, Universidade de Lisboa, Av. Rovisco Pais 1, 1049-001 Lisboa, Portugal

[c]UNIDEMI, Departamento de Engenharia Mecânica e Industrial, Faculdade de Ciências e Tecnologia, Universidade NOVA de Lisboa, Campus Universitário, Caparica, Portugal

[d]Centro Láser UPM, Universidad Politécnica de Madrid, C/ de Alan Turing, 1, 28031 Madrid, Spain
✉Corresponding author: jgomes@deq.isel.ipl.pt

Submitted: 25 March 2017; Accepted: 12 May 2017; Available On-line: 27 November 2017

ABSTRACT: This paper describes an experimental study on the emission of nanometric size particles during laser shock processing of metallic materials: stainless steel, aluminum and titanium alloys which are the most common ones processed by this technique. The emission of nanometric size particles was confirmed to consist of aggregates composed of smaller spherical particles in the range of 10-20 nm, covered by a small concentric "layer" probably of metal oxides. The analysis of the nanoparticles showed the presence of the main elements present in the tested alloys as well as high oxygen content, which is another indication of the presence of oxides of Fe, Al and Ti. The amount of emitted nanoparticles, showed considerable increases over the baseline measured for the working envi-ronment, and these increases correspond to the more intense pulses of the laser beam. The material density was seen to highly affect the quantity of emitted nanoparticles. During LSP of aluminium alloy (the lighter material) a large quantity of nanoparticles was measured, while in LSP of stainless steel few nanoparticles were observed, and this is the denser material, among the three tested. Titanium alloy results in intermediate values. The study of these emissions is innovative and relevant for industrial environments where the manufacturing process is in use.

KEYWORDS: AA6061; AISI304; Laser shock peening; Nanoparticles; Ti6Al4V

Citation/Citar como: Gomez, J.F.; Miranda, R.M.; Porro, J.A.; Ocaña, J.L. (2017) "Experimental characterization of nanoparticles emissions during Laser Shock Processing of AA6061, AISI304 and Ti6Al4V". *Rev. Metal.* 53 (4):e104. http://dx.doi.org/10.3989/revmetalm.104

RESUMEN: *Caracterización experimental de las emisiones de nanopartículas en el tratamiento de AA6061, AISI304 y Ti6Al4V por ondas de choque generadas por LASER*. Este artículo es un estudio experimental sobre la caracterización de las emisiones de nanopartículas en el tratamiento superficial por ondas de choque generadas por LASER (LSP) de materiales metálicos: aceros inoxidables, aleaciones de aluminio y de titanio. Se confirmó que la emisión de partículas de tamaño nanométrico consiste en agregados compuestos de partículas esféricas en el rango de 10-20 nm, cubiertas por una pequeña "capa" concéntrica correspondiente a óxidos metálicos. El análisis de las nanopartículas mostró la presencia de los principales elementos presentes en las aleaciones ensaya-das, y también un contenido elevado de oxígeno que corrobora la presencia de óxidos de Fe, Al y Ti. La cantidad de nanopartículas emitidas, mostró aumentos considerables sobre la línea de base medida para el ambiente de trabajo, y estos aumentos corresponden a los impulsos más intensos de LASER. Se observó que la densidad del

material influí en la cantidad de nanopartículas emitidas. Durante el LSP de aleación de aluminio (el material más ligero) se midió una gran cantidad de nanopartículas, mientras que en LSP de acero inoxidable se observaron pocas nanopartículas, y este es el material más denso, entre los tres ensayados. La aleación de titanio da como resultado valores intermedios. El estudio de estas emisiones es innovador y relevante para entornos industriales donde el proceso de fabricación está en uso.

PALABRAS CLAVE: AA6061; AISI304; Nanopartículas; Ondas de choque generadas por Láser; Ti6Al4V

ORCID ID: João F. Pereira Gomes (http://orcid.org/0000-0003-2579-6669); Rosa M. Mendes Miranda (http://orcid.org/0000-0002-6551-9677); Juan A. Porro Gonzalez (http://orcid.org/0000-0001-5260-527X); José L. Ocãna Moreno (http://orcid.org/0000-0001-9263-8404)

1. INTRODUCTION

Laser shock processing (LSP) is a recently developed technique for surface treatment, among the different methods currently used for improving superficial metallic properties surface by using high density beams, that has proved to be quite effective for improving the fatigue properties of several metals and alloys (Rubio-Gonzalez *et al.*, 2004), due to its ability to induce metallurgical transformations providing enhanced material resistance in terms of fatigue and stress corrosion cracking (Ocaña *et al.*, 2004). This technique was initially developed bearing in mind the critical aeronautic industrial applications resulting in an improvement of the fatigue cracking resistance of materials used. Nowadays, materials such as titanium and aluminium alloys, as well as some types of stainless steels have been thoroughly investigated. However, the unavailability of equipment capable to deliver the needed laser beam intensities has prevented generalized implementation at an industrial level. Recently, powerful laser sources delivering beam power densities exceeding 1 $W.cm^{-2}$, allowed a more generalized application of LSP technology in industry.

Laser Shock Processing consists on applying a high intensity pulsed laser beam having a power density above 10^9 $W.cm^{-2}$ and pulse durations below 50 ns, on a target made of metal, that will result in producing a quick vaporization on its surface immediately developing a high temperature density plasma which creates a shock wave that will propagate to the material itself.

In an initial stage (with the laser beam being quite active on the component itself), the energy from the laser will be deposited on the interface between the metallic target and its surrounding environment (usually formed by a transparent confining material). Therefore, the pressure that is generated by the plasma produces two shock waves that will propagate in two opposite directions, respectively inside the target and to the confining material. As a result of the material motion produced by the two shock waves, an opening of the interface takes place, thus resulting in its widening. Even if the laser is switched off, the plasma will continue to maintain a certain level of pressure, thus decreasing while expanding as a result of the increase of the plasma volume. After plasma recombination is completed, a projectile-like expansion of the heated gas inside the interface results in an additional mechanical momentum to the target. A process scheme is shown in Fig. 1.

Then, the treated material experiences a permanent deformation as a result of the pressure induced by the laser generated shock wave, and this has to be optimized for certain laser characteristics, such as pulse duration, wavelength and power density, laser spot size, bearing in mind the thickness and composition of the coating/confining materials. The description of the relevant laser absorption phenomena is hardly complex as it results from non-linear effects appearing along the interaction process that significantly alter the shocking dynamics, and also because of the need to describe the laser induced shock waves propagation in solid materials. Therefore, the plasma formation deriving from the laser-material interaction is a rather complex phenomena.

In addition to the LSP physical aspects relating to the generation and propagation of the shock waves transforming the target material, attention has to be given to the emission of nanoparticles during the process, following other similar studies performed on materials processing techniques such as surface processing and welding, aiming at the need to guarantee a safe workplace environment for operators (Buonanno *et al.*, 2011; Tsai *et al.*, 2011). The knowledge on the level of nanoparticles emitted during those processes is fundamental in order

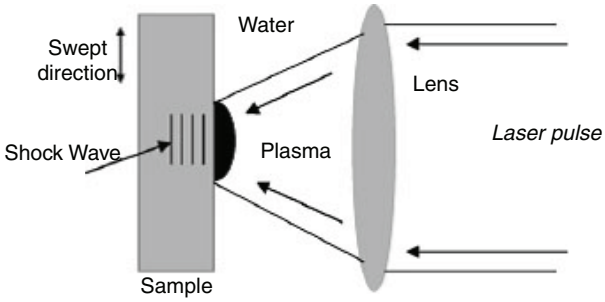

FIGURE 1. Laser shock processing principle.

to be able to derive effective protection measures (Guerreiro *et al.*, 2014; Albuquerque *et al.*, 2015), so that the occupational exposure during industrial operations can be rather limited, thus contributing for a less harmful workplace environment.

Additionally, although the effect can be minimized by the adoption of mitigation techniques, nanoparticle emissions can affect the homogeneity of the treated surfaces since they can damage either the optical system or accumulate in the surroundings of the local processed zone.

In this study, an analysis was performed aiming at evaluating the nanoparticles emission in Laser Shock Processing conditions of representative materials used in industry.

2. MATERIALS AND METHODS

2.1. Laser processing conditions

The LSP trials were done by using a Q switched Nd:YAG laser operating at 10 Hz and having a wavelength of 1064 nm, whereas the full width at half maximum (FWHM) pulse was of 10 ns. A convergent lens was used to have a beam spot diameter of around 1.5 mm and an energy per spot was of 1.2 J. Pulse density was 289 pulses.cm^{-2}. Metallic specimens (60x60x6.3 mm) were fixed and a 2D robot motion system that was used to control the specimen position and generate the adequate pulse swept as depicted in Fig. 2. The plate rolling direction (L) was perpendicular to sliding direction and also to the LSP swept direction. Water was continuously added as a confining material with a small flow in the interaction zone. No absorptive layers were used during tests.

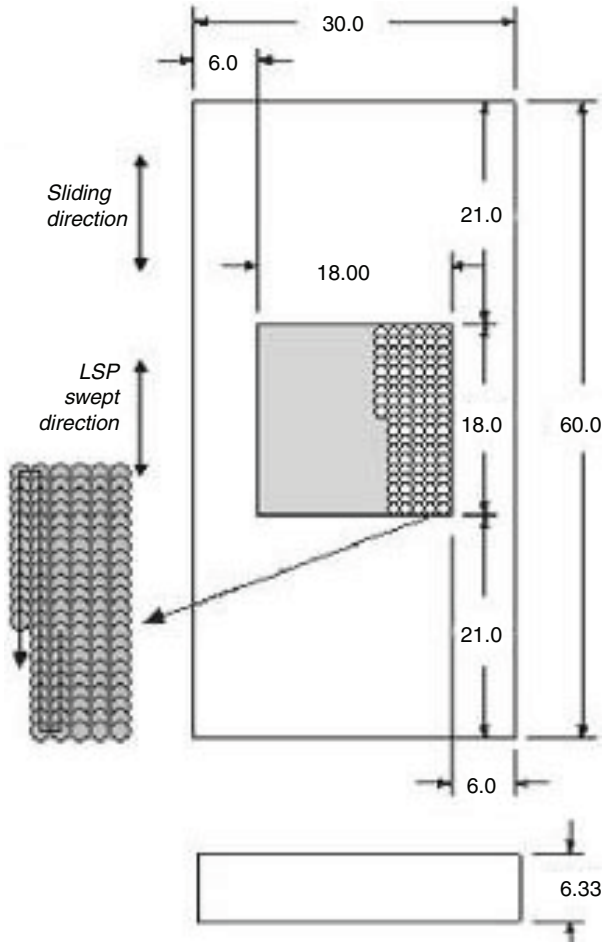

FIGURE 2. Positioning and size of specimens during LSP, indicating also the treated zone and the swept direction.

LSP was performed into three different materials currently processed by this technique in industry: AA 6061-T6, stainless steel AISI 304 and titanium alloy Ti6Al4V. Table 1 shows the chemical composition referred alloys. Tests were made in triplicate, using always the same FWHM pulse and wavelength.

2.2. Airborne nanoparticles measurements

A single point, located immediately above the interaction area between the laser beam and the specimen, where an operator would typically be working in order to control the process was chosen for sampling.

The main characteristic of nanoparticles is that they have a large surface area which increases along with the decrease of particle size for the same amount of mass. In terms of exposure assessment in what regards nanoparticles, the most common

TABLE 1. Chemical composition and specific weight of the alloys tested

Elements	Content (wt. %)		
	AISI304	Al 6061-T6	Ti 6Al4V
Al	-	remaining	6.0
C	< 0.08	-	< 0.10
Cr	18.0-20.0	0.27	-
Cu	-	0.13	-
Fe	remaining	0.27	< 0.3
Mg	-	0.46	-
Mn	< 2.0	0.03	-
Ni	8.0-10.5	-	-
P	< 0.045	-	-
S	< 0.03	-	-
Si	< 1.0	0.52	-
Ti	-	0.022	~ 90.0
V	-	-	4.0
Zn	-	0.11	-
Specific weight (g cm^{-3})	7.93	2.70	4.47

procedure is the determination of the surface area deposited in the human lung (Oberdorster, 2000). A nanoparticle surface area monitor (NSAM) TSI, Mod. 3550 was used, as this equipment is able to estimate the surface area of particles deposited in the alveolar region of the human lung, expressed as square micrometers per cubic centimeter of air ($\mu m^2 cm^{-3}$) referred further on as Alveolar Deposited Surface Area (ADSA), and is used with proved reliability for the size range of particles between 20 and 100 nm (Asbach *et al.*, 2009), which means that the equipment could be operating very near its detection limit. However, Asbach *et al.* (2009) concluded that the fraction below 20 nm usually contributes only negligibly to the total area surface and, therefore, it is not critical.The operation of this equipment is based on diffusion charging of sampled particles (Gomes *et al*., 2012a; Gomes *et al*., 2012b), followed by the detection of the charged aerosol using an electrometer, which uses the deposition model developed by the International Commission on Radiological Protection (ICRP). Also, emitted nanoparticles were collected with a Nanometer Aerosol Sampler (NAS) TSI, Mod. 3089 on copper grids, polymer coated, having a diameter of 3 mm for further observation by transmission electron microscopy (TEM). For these a TEM Hitachi, Mod. H-8100 II, and an energy dispersive X-ray spectroscopy (EDS) probe, were used, as described elsewhere (Gomes *et al.*, 2013).

3. RESULTS AND DISCUSSION

3.1. Exposure assessment

The tests on each material consisted on the measurement of ADSA of emitted nanoparticles. During tests replicates were done and were generally in reasonable agreement. Therefore, the results presented in Table 2 show peaks calculated from the average values measured, comprising replicates. Prior to these measurements, a baseline was obtained corresponding to an averaged ADSA value of 16.5 μm^2 cm^{-3}. Table 2 indicates also the percentage increase of ADSA over the measured baseline.

Figures 3, 4 and 5 show the evolution of ADSA values during tests for each material under study, whereas Fig. 6 shows the accumulated ADSA if the three tests (one for each alloy) were made in sequence, simulating the total exposure experienced by an operator, working in a typical industry processing parts of different alloys in sequence. For this hypothetical situation, the accumulated values, as well as the statistic parameters, are presented in Table 3, together with a calculated a threshold value (TWA-Time Weighted Average) for an exposure of 8 h, and also the dose per lung of worker, accounting for a typical area of human lung of 80 m^2 (Phallen, 1999). The dose per lung is calculated dividing the total ADSA per the lung area.

During individual tests, for the different materials, some peaks could be observed corresponding to the higher pulses of the laser beam. In terms of maximum measured ADSA values, it can be noticed that the highest values correspond to the aluminium alloy, which is the least dense material, and the lowest were measured for stainless steel which is the denser material, amongst the three tested. Titanium alloy shows intermediate values of ADSA.

Nevertheless, the measured ADSA values represent a very significant increase over the baseline. Also, the calculated TWA for 8 h, considering that tests for the 3 alloys were done in sequence, show a high value and an important dose per worker's lung, which calls for the adoption of effective protective measures considering both worker's exposure and process homogeneity.

3.2. Size distribution of emitted nanoparticles

Figures 7, 8 and 9 show micrographs, obtained by TEM of nanoparticles captured during the LSP tests. Particles are clearly in the nano range, forming agglomerates composed of smaller spherical particles. Individual nanoparticles are in the range of 10-20 nm. Nevertheless, it should be taken into consideration that the used NSAM equipment provides reliable measurements in the size range of 20-400 nm, which means that the equipment is operating very near its detection limit. However, Asbach *et al.* (2009) concluded that the fraction below 20 nm usually contributes only negligibly to the total area surface and, therefore, it is not critical. It can be noticed that some of the particles are covered by a small concentric "layers" probably of metal oxides of the metals detected, e.g. Al, Fe and Ti.

TABLE 2. Maximum averaged ADSA measured for the alloys tested

Alloys	Max ADSA (μm^2 cm^{-3})	Increase over the baseline (%)
AISI 304	14700	89.0×10^3
Al 6061-T6	98700	598.1×10^3
Ti6Al4V	48800	295.7×10^3

TABLE 3. Accumulated calculated ADSA values for 3 tests in sequence

Parameters	Max ADSA (μm^2 cm^{-3})
Averaged ADSA	10,000
Standard deviation	21,500
TWA for 8 h	917.2
Accumulated ADSA	4.40×10^8 μm^2
Dose per lung	5.50×10^6 μm^2

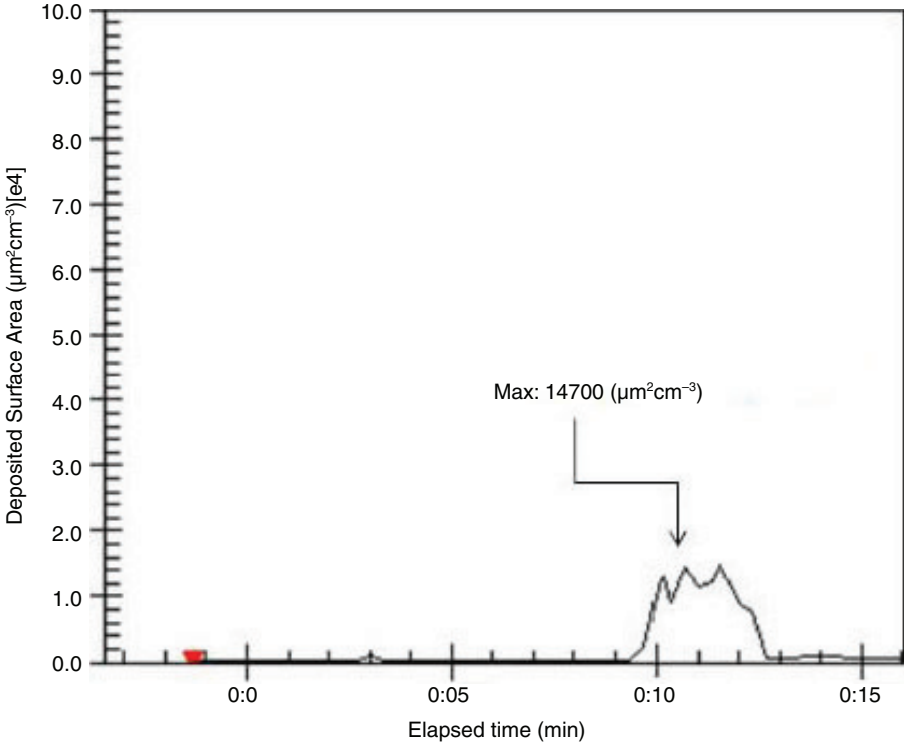

FIGURE 3. Averaged ADSA measurements obtained for stainless steel AISI 304.

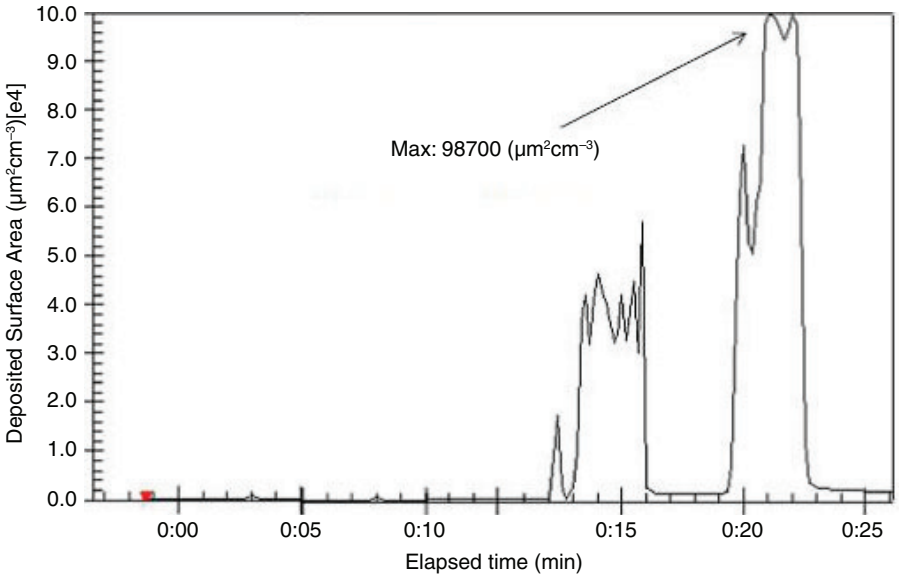

FIGURE 4. Averaged ADSA measurements obtained for aluminum alloy 6061-T6.

3.3. Morphology and chemical composition of emitted nanoparticles

Collected nanoparticles were also analysed for determination chemical composition by EDS. Figures 10, 11 and 12 shows the EDS spectra obtained for LSP tests with stainless steel, aluminium alloy and titanium alloy, respectively.

Regarding stainless steel, main elements present in the nanoparticles are, Cr and Fe, which are the elements present in more content in the steel. Ni is denser than the others, but is in the alloy in a small volume

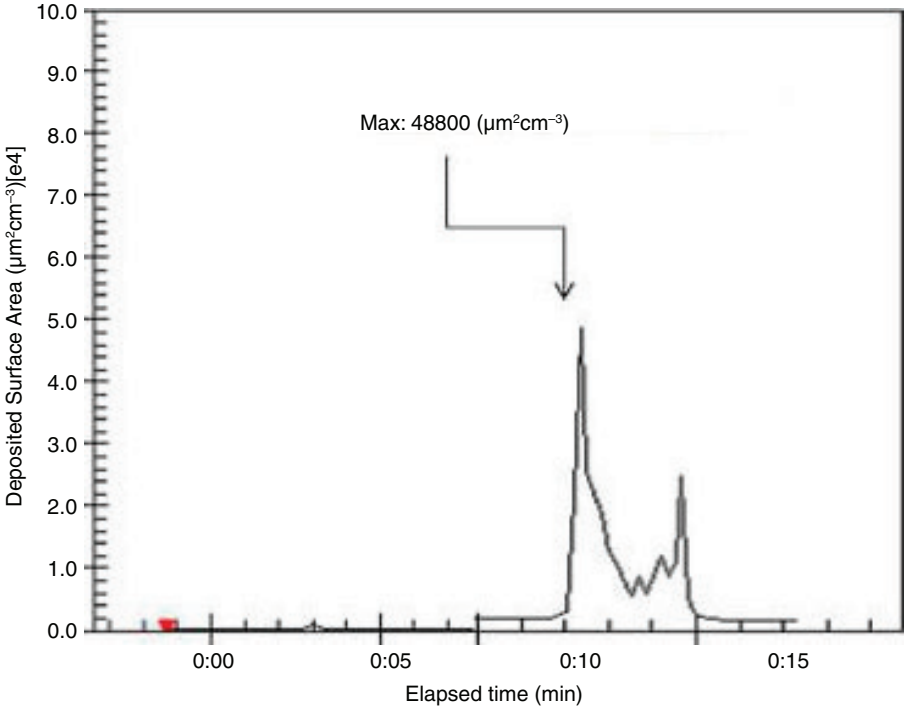

FIGURE 5. Averaged ADSA measurements obtained for titanium alloy 6Al4V.

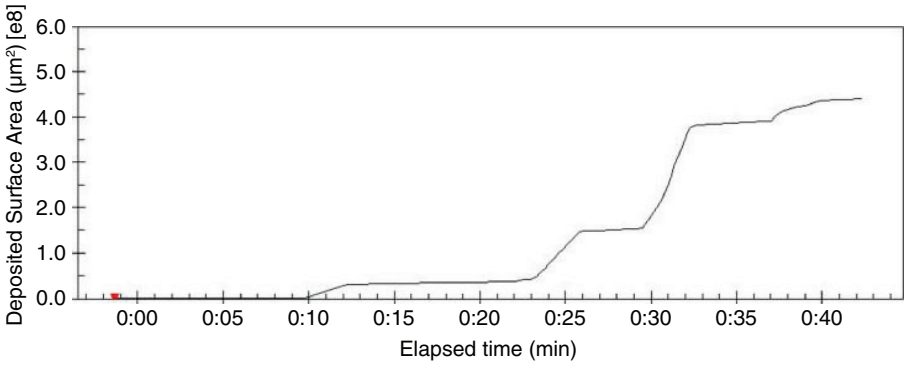

FIGURE 6. Accumulated averaged ADSA for 3 metals, if sequentially made.

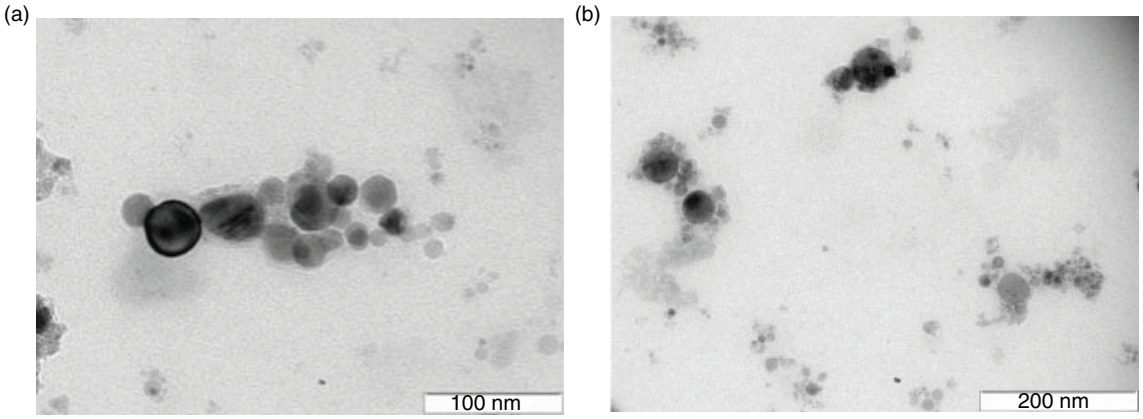

FIGURE 7. Images of nanoparticles collected during LSP tests in AISI 304 observed by TEM.

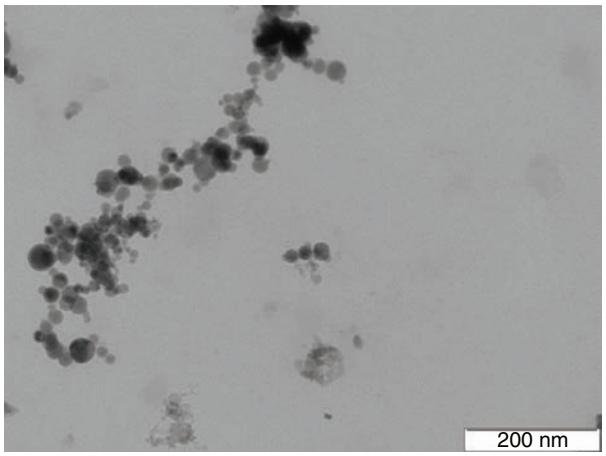

FIGURE 8. Image of nanoparticles collected during LSP tests in AA 6061-T6 observed by TEM.

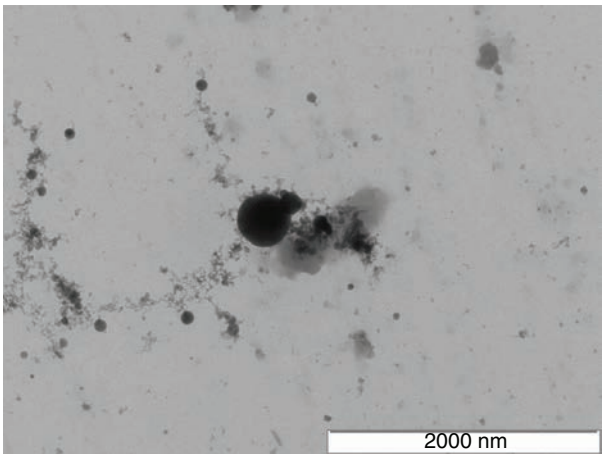

FIGURE 9. Image of nanoparticles collected during LSP tests in Ti6Al4V observed by TEM.

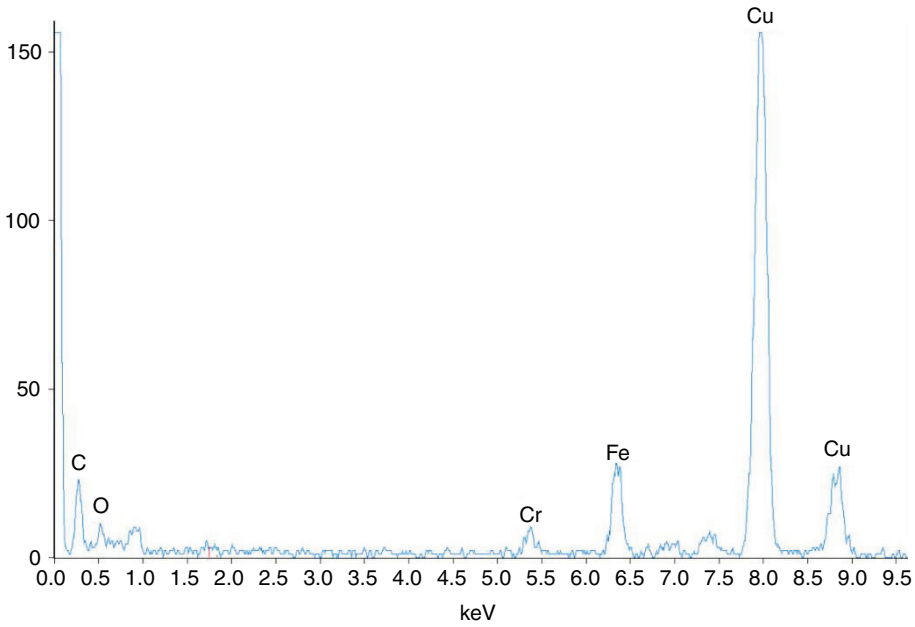

FIGURE 10. EDS spectra of particles collected during measurements for stainless steel AISI 304.

percentage. Nanoparticles released during aluminium alloy LSP tests mainly show the presence of Al, despite the fact that this is denser than Mg and Si which are the alloying elements in AA6xxx series but are present in minor content. Nanoparticles released during LSP of Ti6Al4V show the presence of Ti and Al. V is denser than the other ones and in less content.

This analysis allows to ascertain the nature of the released nanoparticles to the nature of the base materials tested, as expected. It can be seen that both the content and the density of the alloying elements affect the nanoparticles emitted. Obtained spectra always exhibit peaks corresponding to copper from the collecting support a grid, which is not coming from the sampled nanoparticles itself. Also, it should be noted the exceptional high content of oxygen detected in each analysis, as can depicted in Figs. 10 to 12. This is an indicator that the observed layers detected correspond to metal oxides of Fe, Al and Ti, respectively.

4. CONCLUSIONS

- This study shows the existence of non-negligible particles emission in the nanometric range during laser shock processing of common alloys used in industry for improving surface properties. Collected particles are mainly aggregates composed of smaller spherical particles in the range of 10-20 nm, covered by a small concentric "layer", probably of metal oxides. EDS analysis of the nanoparticles showed the presence of the

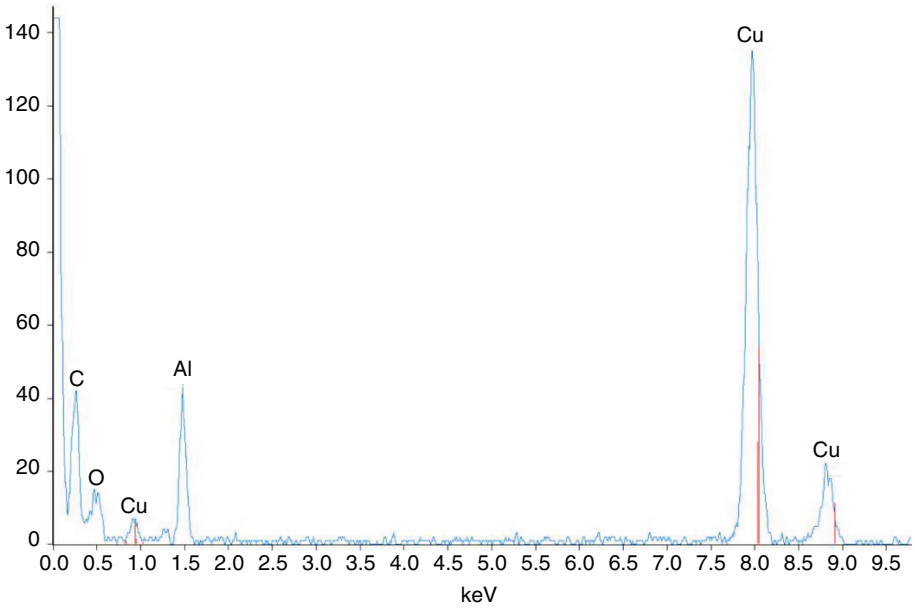

FIGURE 11. EDS spectra of particles collected during measurements for aluminum alloy 6061-T6.

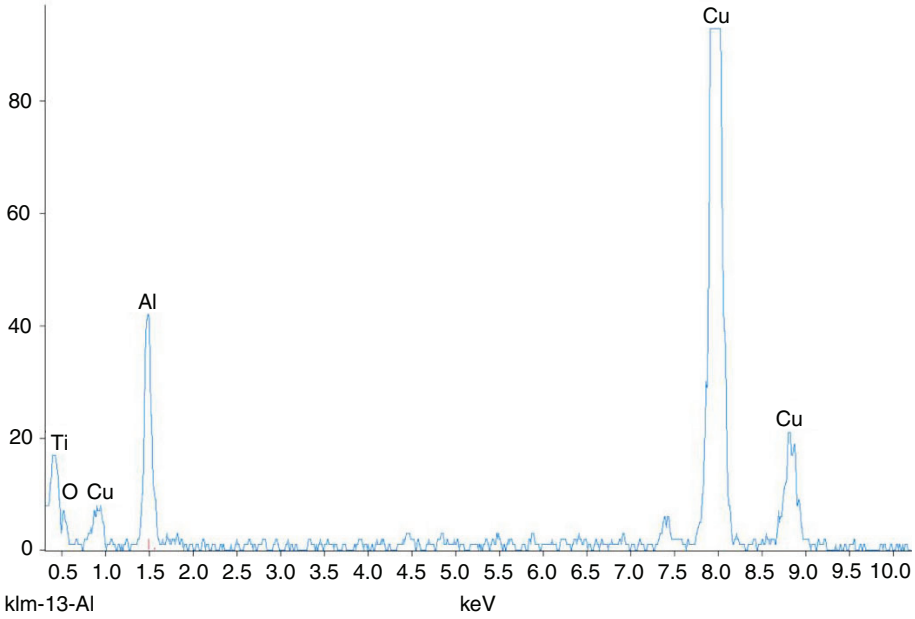

FIGURE 12. EDS spectra of particles collected during processing of Ti6Al4V.

main elements present in the tested alloys, as well as a high oxygen content, which is another indication of the presence of oxides of Fe, Al and Ti.

- The amount of emitted nanoparticles, measured by ADSA showed considerable increases over the baseline measured for the working environment, and the observed ADSA peaks correspond to the higher pulses of the laser beam. The highest density of nanoparticles was observed in LSP of the aluminum alloy, which is also the least dense material, and the lowest were measured for stainless steel which is the more dense material, among the three tested.
- Titanium alloy results in intermediate values of ADSA, being the material with the intermediate density. The calculated Time Weighted Average

for 8 h working time, considering that tests for the 3 alloys are done in sequence, show a considerable high value and an important dose per worker's lung, which calls for the adoption of effective protective measures considering worker's exposure, such as containment measures and/or the use of effective individual protection devices for particles in the nano size range.

REFERENCES

Albuquerque, P.C., Gomes, J.F., Pereira, C.A., Miranda, R.M. (2015). Assessment and control of nanoparticles exposure in welding operations by use of a Control Banding Tool. *J. Clean. Prod.* 89, 296–300. http://dx.doi.org/10.1016/j.jclepro.2014.11.010.

Asbach, C., Fissan, H., Stahlmecke, B., Kuhlbusch, T., Pui, D. (2009). Conceptual limitations and extensions of lung-deposited Nanoparticle Surface Area Monitor (NSAM). *J. Nanopart. Res.* 11 (1), 101–109. http://dx.doi.org/10.1007/s11051-008-9479-8.

Buonanno, G., Morawska, L., Stabile, L. (2011). Exposure to welding particles in automotive plants. *J. Aerosol Sci.* 42 (5), 295–304. http://dx.doi.org/10.1016/j.jaerosci.2011.02.003.

Gomes, J., Albuquerque, P., Miranda, R.M., Vieira, M.T. (2012a). Determination of Airborne Nanoparticles from Welding Operations. *J. Toxicol. Env. Heal. A* 75 (13-15), 747–755. http://dx.doi.org/10.1080/15287394.2012.688489.

Gomes, J., Albuquerque, P., Miranda, R., Santos, T., Vieira, M.T. (2012b). Comparison of deposited surface area of airborne ultrafine particles generated from two welding processes. *Inhal. Toxicol.* 24 (11), 774–781. http://dx.doi.org/10.3109/08958378.2012.717648.

Gomes, J., Guerreiro, C., Lavrador, D., Carvalho, P., Miranda, R.M. (2013). TEM analysis as a tool for toxicological assessment of occupational exposure to airborne nanoparticles from welding. *Microsc. Microanal.* 19 (S4), 153–154. http://dx.doi.org/10.1017/S1431927613001384.

Guerreiro, C., Gomes, J.F.P., Carvalho, P., Santos, T., Miranda, R.M., Albuquerque, P. (2014). Characterisation of airborne particles generated from metal active gas welding process. *Inhal. Toxicol.* 26 (6), 345–352. http://dx.doi.org/10.3109/08958378.2014.897400.

Oberdorster, G. (2000). Pulmonary effects of inhaled ultrafine particles. *Int. Arch. Occ. Env. Hea.* 74 (1), 1–8. http://dx.doi.org/10.1007/s004200000185.

Ocaña, J., Molpeceres, C., Porro, J., Gomez, G., Morales, M. (2004). Experimental assessment of the influence of irradiation parameters on surface deformation and residual stresses in laser shock processed metallic alloys. *Appl. Surf. Sci.* 238 (1-4), 501–505. http://dx.doi.org/10.1016/j.apsusc.2004.05.246.

Phallen, R. (1999). *Particle size-slective sampling for particulate air contaminants*. Ed. J. H. Vincent, ACGIH, Cincinnati, OH, USA.

Rubio-Gonzalez, C., Ocaña, J., Gomez-Rosas, G., Molpeceres, C., Paredes, M., Banderas, A., Porro, J., Morales, M. (2004). Effect of laser shock processing on fatigue crack growth and fracture toughness of 6061-T6 aluminum alloy. *Mat. Sci. Eng. A-Struct.* 386 (1-2), 291–295. http://dx.doi.org/10.1016/j.msea.2004.07.025.

Tsai, C., Huang, C., Chen, S., Ho, C., Huang, C., Chen, C., Cheng, C., Tsai, S., Ellenbecker, M. (2011). Exposure assessment of nano-sized and respirable particles at different workplaces. *J. Nanopart. Res.* 13 (9), 4161–4172. http://dx.doi.org/10.1007/s11051-011-0361-8.